τ Decay Mode Identification in a Liquid Argon Electromagnetic Calorimeter at the FCC-ee

Katinka Wandall-Christensen

Supervisor:
Mogens Dam

Niels Bohr Institute
University of Copenhagen

27 January 2022

Introduction

τ polarisation measurements

Motivation:

Improving the precision of $\sin^2(\theta_W)$ and testing the $e - \tau$ universality

τ polarisation measurements

Motivation:

Improving the precision of $\sin^2(\theta_W)$ and testing the $e - \tau$ universality

Requirements:

- Precision measurements

$\Rightarrow$ Need a clean and precise separation of τ final states

- Largest sensitivity to polarisation in $\pi\, n\pi^0$ modes, with $n \geq 0$. In particular the $\pi^-\nu$ and $\rho^-\nu \to \pi^-\pi^0\nu$ have the largest sensitivities to P_τ

Decay modes	Branching fraction [%]
$e^-\, \bar{\nu}_e\, \nu_\tau$	17.82 ± 0.04
$\mu^-\, \bar{\nu}_\mu\, \nu_\tau$	17.39 ± 0.04
$h^-\, \nu_\tau$	11.51 ± 0.05
$h^-\, \pi^0\, \nu_\tau$	25.93 ± 0.09
$h^-\, 2\pi^0\, \nu_\tau$	9.48 ± 0.10
$h^-\, 3\pi^0\, \nu_\tau$	1.18 ± 0.07
$h^-\, 4\pi^0\, \nu_\tau$	0.16 ± 0.04
3 prongs	15.20 ± 0.06

Table: The dominant decay modes and their branching fractions of the τ lepton. h^- represents a K^- or a π^-

$\Rightarrow$ Need a precise π^0 counting scheme

Project goal

Investigate the performance of the LAr/Pb ECAL proposed for the FCC-ee wrt. τ polarisation measurements by trying to achieve the best possible τ decay mode identification. This demands:

- A precise π^0 reconstruction scheme
- A separation of single γ and merged π^0's

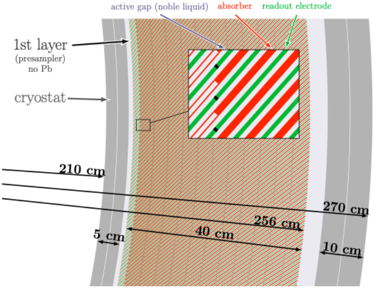

Figure: The proposed LAr/Pb ECAL barrel design [arXiv:2109.00391]

Detector demands

- Sensitivity to low energy photons. This includes a minimization of noise to enhance precision in π^0 counting
- High granularity to detect both π^0 daughter photons

  Angle between two photons of equal energy:

$$\alpha(\gamma,\gamma) = \frac{m_{\gamma,\gamma}}{E_\gamma} \quad (1)$$

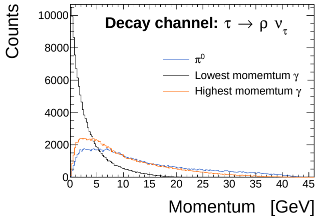

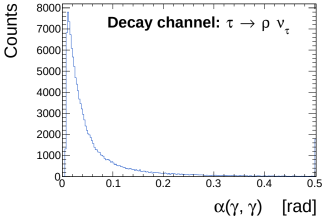

Electromagnetic showers:

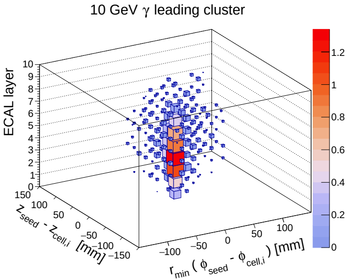

Figure: Cluster from 10 GeV photon in the LAr ECAL

- Mostly regular in shape
- Molière radius (R_M): Radius of cylinder on avg. containing 90% of shower (material dependent)

Hadronic showers:

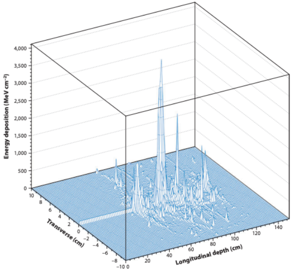

Figure: 100 GeV pion creating a hadronic shower in Pb [10.1146/annurev.nucl.012809.104449]

- Initial MIP behaviour
- Cascades of secondary particles → irregular shape with satellites

Simulations

Simulated geometry

Simplified geometry:

- 70 concentric cylinders
- PCB simulated by making glue layer thicker and an average material constant is used

- Depth: $20.6X_0$

Event files:

- Single particle gun. Particles generated at $\phi = 0$, $\theta = \frac{\pi}{2}$
- Full τ decay. Produced at $\theta = \frac{\pi}{2}$.

$\Rightarrow$ All Geant4 hits saved to root output file

DISCLAIMER

It was discovered late in the thesis process that the intermediate ρ meson or a_1 is not produced

Consequences for $\tau \to \rho\nu$ decays:

- 3-body decay instead of 2-body $\to$ enhanced $\alpha(\pi^{\pm}, \gamma)$
- Momentum distributions of $\pi^{\pm}$ and π^0 slightly different

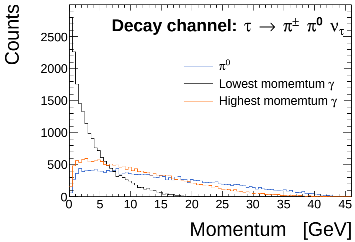

However, the π^0 decays happen realistically

Geant4 hits to cell hits

- Calorimeter divided into 10 layers in the r-direction, 680 cells in ϕ-direction and 300 cells in $z-$direction
- Cell size: $\sim 2 \times 2 \times 4\ \mathrm{cm}^3$
- All geant hits are assigned a cell
- Illuminate evenly over cell surface: position of entire event displaced randomly within the area of one cell

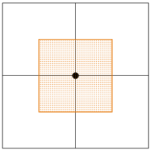

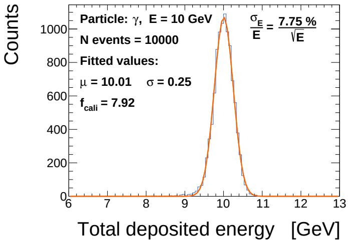

Sampling fraction: 12.6%

A liquid krypton/tungsten design

LKr and W have smaller Molière radii → possible better separation of close-by photons.

- LAr/Pb replaced by LKr/W
- 70 concentric cylinders
- Layer thickness reduced to 3.7 mm → 140 mm narrower ECAL
- Depth: $21.3X_0$
- Calorimeter divided into 10 layers in the r-direction, 1360 cells in ϕ-direction and 600 cells in $z-$direction
- Cell size: $\sim 1 \times 1 \times 2.6 \text{ cm}^3$

Comparison using Geant4 hits

LAr design:

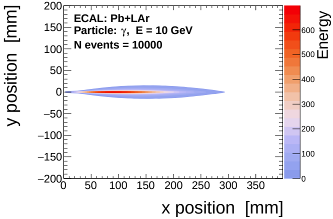

$R_M = 41$ mm

LKr design:

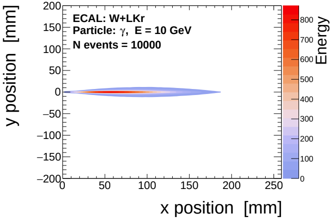

$R_M = 27$ mm

$\Rightarrow$ LKr design does give narrower showers

Shower reconstruction

Clustering algorithm

Methods uses two (adjustable) thresholds: $\mathrm{thrs}_{low} = 10$ MeV, $\mathrm{thrs}_{high} = 20$ MeV

Clustering algorithm

Methods uses two (adjustable) thresholds: $\text{thrs}_{low} = 10$ MeV, $\text{thrs}_{high} = 20$ MeV

1. For each cell, point to highest energy (of 26) neighbours exceeding thrs_{low}
   - If the cell is local maximum and exceeds thrs_{high} it will be a seed
   - For each cell, define list of followers (cells that point to it)

Clustering algorithm

Methods uses two (adjustable) thresholds: $\mathrm{thrs}_{low} = 10$ MeV, $\mathrm{thrs}_{high} = 20$ MeV

1. For each cell, point to highest energy (of 26) neighbours exceeding thrs_{low}
   - If the cell is local maximum and exceeds thrs_{high} it will be a seed
   - For each cell, define list of followers (cells that point to it)
2. Start by seed cells (local energy maximum) and collect followers iteratively $\rightarrow$ proto-clusters

Clustering algorithm

Methods uses two (adjustable) thresholds: $\mathrm{thrs}_{low} = 10$ MeV, $\mathrm{thrs}_{high} = 20$ MeV

1. For each cell, point to highest energy (of 26) neighbours exceeding thrs_{low}
   - If the cell is local maximum and exceeds thrs_{high} it will be a seed
   - For each cell, define list of followers (cells that point to it)
2. Start by seed cells (local energy maximum) and collect followers iteratively $\rightarrow$ proto-clusters
3. Merging of proto-clusters

Clustering algorithm

Methods uses two (adjustable) thresholds: $\mathrm{thrs}_{low} = 10$ MeV, $\mathrm{thrs}_{high} = 20$ MeV

1. For each cell, point to highest energy (of 26) neighbours exceeding thrs_{low}
   - If the cell is local maximum and exceeds thrs_{high} it will be a seed
   - For each cell, define list of followers (cells that point to it)
2. Start by seed cells (local energy maximum) and collect followers iteratively $\rightarrow$ proto-clusters
3. Merging of proto-clusters

$\Rightarrow$ A reconstruction threshold of $E_{clus} > 200$ MeV is used

Clustering - 10 GeV photons

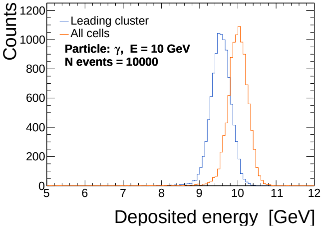

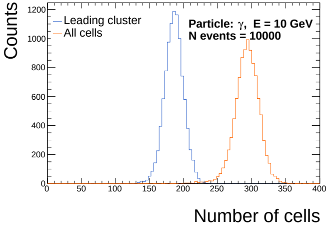

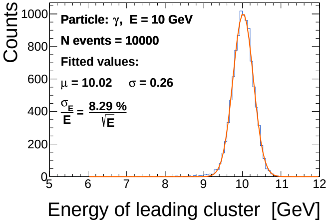

- Leading cluster contains majority of particle energy
- Energy resolution slightly reduced

⇒ successful clustering

Clustering - 10 GeV photons

Position resolution:

- The cluster positions are calculated as the energy weighted mean of the associated cell positions

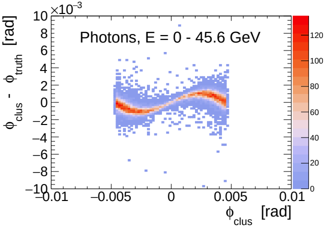

Figure: ϕ coordinate

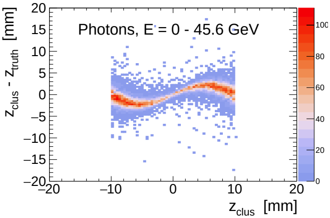

Figure: z coordinate

$\Rightarrow$ need an s-curve correction

S-curve correction - 10 GeV photons

Correction is done by fitting a sine function to s-curves and using the fit result as the correction

Result:

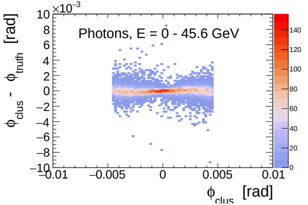

Figure: ϕ coordinate

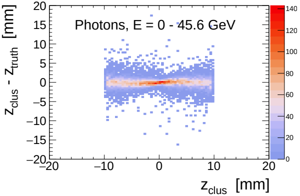

Figure: z coordinate

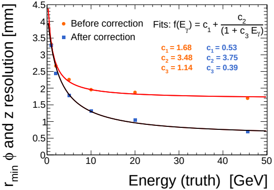

$\Rightarrow r\phi/z$ resolution for 10 GeV photons at $r = 2160$ mm: 1.95 mm (before) $\rightarrow$ 1.28 mm (after)

Introduction

Simulations

Shower reconstruction

Particle identification

Results

Comparing LAr/LKr ECAL designs

Conclusion

Clustering - 10 GeV charged pions

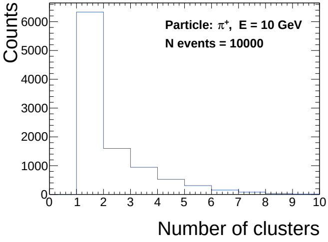

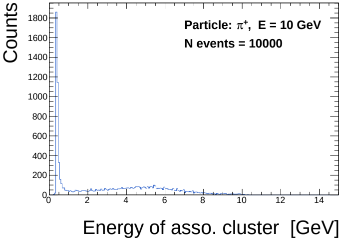

- On average 0.8 additional clusters per generated 10 GeV particle
- Associated cluster chosen based on proximity to charged track

$\Rightarrow$ need a fake photon killing to separate genuine/fake photons

Clustering - π^0's

$\alpha(\gamma, \gamma) \propto \frac{1}{E_\pi^0}$

$\Rightarrow$ daughter photons from high energy π^0 are likely to merge into one cluster

Clustering - π^0's

$\alpha(\gamma, \gamma) \propto \frac{1}{E_\pi^0}$

$\Rightarrow$ daughter photons from high energy π^0 are likely to merge into one cluster

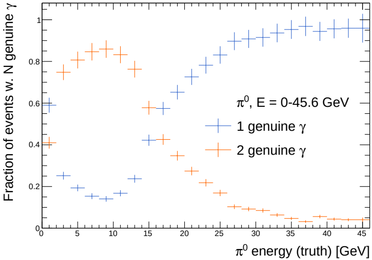

- Resolved π^0's: The two photons are reconstructed as two separate clusters
- Unresolved π^0's: The two photons merge into one cluster
- Residual single photons: One photon is under reconstruction threshold

Particle identification

Fake photon killing

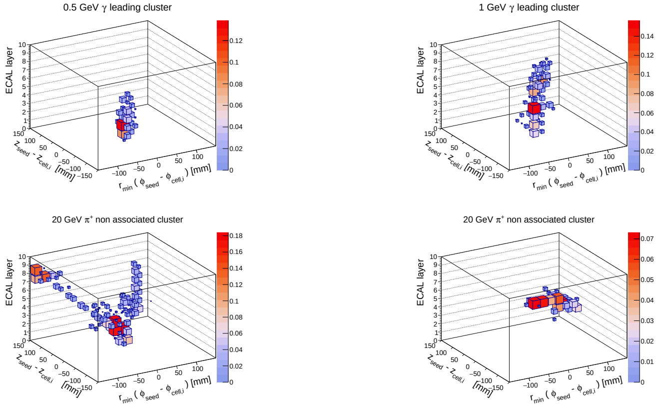

$\Rightarrow$ fakes per $\pi^{\pm}$ reduced by a factor 26 to 0.035 fakes per $\pi^{\pm}$

Single photon/unresolved π^0 separation

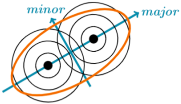

$\Rightarrow$ Major axis correlated with opening angle of photons

Single photon/unresolved π^0 separation

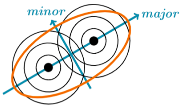

$\Rightarrow$ Major axis correlated with opening angle of photons

The major/minor axis lengths can be re-formulated to calculate a cluster mass:

$$m_{\text{clus}} = c_1 E_{\text{clus}} x \qquad (2)$$

with

$$x^2 = major^2 - minor^2 \, . \qquad (3)$$

Calibration factor: $c_1 \sim 1$.

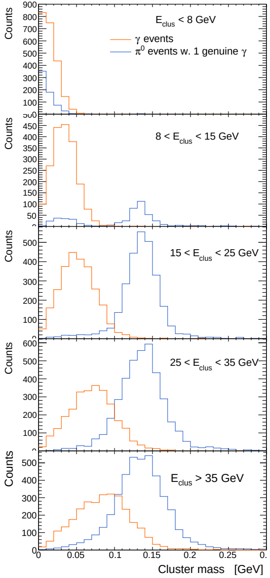

Results

π^0 reconstruction

1. Combine all genuine photons to find resolved π^0's
   - Photon pair accepted if $m_{\gamma,\gamma}$ is consistent with m_{π^0} within $4\sigma_{m_{\gamma,\gamma}}$

   $\Rightarrow$ $\epsilon_{E<16\mathrm{GeV}} > 98\%$

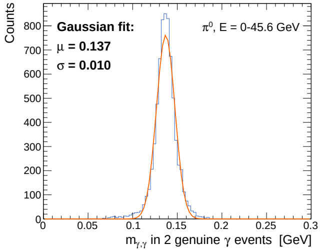

π^0 reconstruction

1. Combine all genuine photons to find resolved π^0's
   - Photon pair accepted if $m_{\gamma,\gamma}$ is consistent with m_{π^0} within $4\sigma_{m_{\gamma,\gamma}}$

   $\Rightarrow$ $\epsilon_{E<16\text{GeV}} > 98\%$

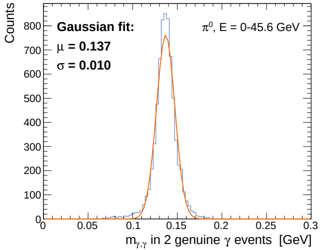

2. Identify all unresolved π^0's
   - Cluster accepted as unresolved π^0 if $m_{clus} > 0.1$ GeV

   $\Rightarrow$ $\epsilon_{E>16\text{GeV}} = 82 - 90\%$, with efficiency decreasing at higher energies

π^0 reconstruction

1. Combine all genuine photons to find resolved π^0's
   - Photon pair accepted if $m_{\gamma,\gamma}$ is consistent with m_{π^0} within $4\sigma_{m_{\gamma,\gamma}}$

   $\Rightarrow$ $\epsilon_{E<16\text{GeV}} > 98\%$

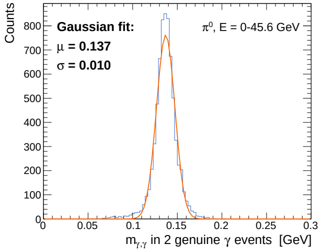

2. Identify all unresolved π^0's
   - Cluster accepted as unresolved π^0 if $m_{clus} > 0.1$ GeV

   $\Rightarrow$ $\epsilon_{E>16\text{GeV}} = 82 - 90\%$, with efficiency decreasing at higher energies

3. Accept remaining genuine photons as residual single photons if $\alpha(\pi^{\pm}, \gamma) < 0.3$ rad

π^0 reconstruction

Signal:

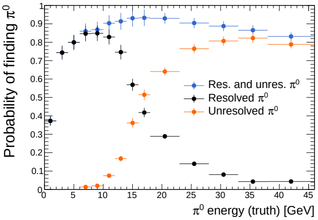

Background:

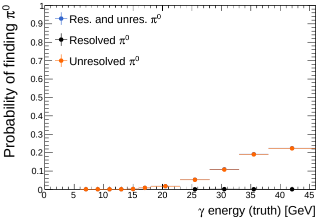

$\Rightarrow$ Probability of reconstructing π^0: $\epsilon = 84\%$ which is competitive with ALEPH results of $\epsilon_{ALPEH} \sim 84\%$ (including residual single photons)
$\Rightarrow$ Probability of accepting a true γ as π^0: $\epsilon_{bg} = 4.5\%$ heavily dominated by photons with $E > 25$ GeV

τ decay mode identification

This thesis:

Recon → / Gen ↓	$\pi^{\pm}\nu$	$\pi^{\pm}\pi^{0}\nu$	$\pi^{\pm}2\pi^{0}\nu$	$\pi^{\pm}3\pi^{0}\nu$	$\pi^{\pm}4\pi^{0}\nu$
$\pi^{\pm}\nu$	**0.9560**	0.0425	0.0010	0.0003	0.0002
$\pi^{\pm}\pi^{0}\nu$	0.0374	**0.9020**	0.0586	0.0016	0.0002
$\pi^{\pm}2\pi^{0}\nu$	0.0090	0.1277	**0.7802**	0.0808	0.0022
$\pi^{\pm}3\pi^{0}\nu$	0.0036	0.0372	0.2679	**0.5972**	0.0910

Table: Each row shows the fraction of e.g. $\tau \to \pi^{\pm}\nu$ decays classified as each of the considered channels

- ⇒ Most event classified correctly for all channels
- ⇒ Efficiency especially high for important $\pi^{\pm}\nu$ and $\pi^{\pm}\pi^{0}\nu$ channels
- ⇒ Efficiency decreases with rising number of π^{0}'s
- ⇒ Contributions to migration: Merging of $\pi^{\pm}$ and π^{0} clusters, radiation photons

τ decay mode identification

This thesis:

Recon → / Gen ↓	$\pi^{\pm}\nu$	$\pi^{\pm}\pi^{0}\nu$	$\pi^{\pm}2\pi^{0}\nu$	$\pi^{\pm}3\pi^{0}\nu$	$\pi^{\pm}4\pi^{0}\nu$
$\pi^{\pm}\nu$	**0.9560**	0.0425	0.0010	0.0003	0.0002
$\pi^{\pm}\pi^{0}\nu$	0.0374	**0.9020**	0.0586	0.0016	0.0002
$\pi^{\pm}2\pi^{0}\nu$	0.0090	0.1277	**0.7802**	0.0808	0.0022
$\pi^{\pm}3\pi^{0}\nu$	0.0036	0.0372	0.2679	**0.5972**	0.0910

Table: Each row shows the fraction of e.g. $\tau \to \pi^{\pm}\nu$ decays classified as each of the considered channels

ALEPH results (normalized to 1. by author):

Recon → / Gen ↓	$h\,\nu$	$h\,\pi^{0}\nu$	$h\,2\pi^{0}\nu$	$h\,3\pi^{0}\nu$	$h\,4\pi^{0}\nu$
$h\,\nu$	**0.9270**	0.0670	0.0047	0.0010	0.0003
$h\,\pi^{0}\nu$	0.0457	**0.8756**	0.0728	0.0053	0.0006
$h\,2\pi^{0}\nu$	0.0044	0.1470	**0.7499**	0.0900	0.0087
$h\,3\pi^{0}\nu$	0.0008	0.0288	0.3098	**0.5768**	0.0837

Remember: not apples-to-apples comparison!!

τ decay mode identification

This thesis:

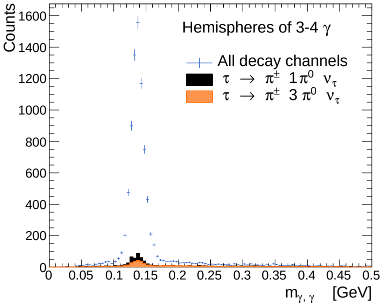

ALEPH results:

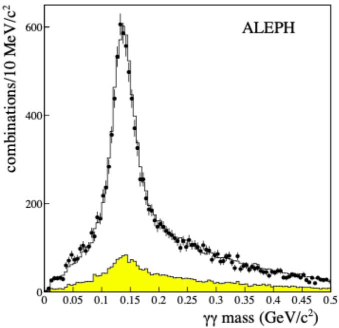

Figures show the invariant mass of two photons in three-four photon events, where one π^0 has already been identified.

Remember: not apples-to-apples comparison!!

Comparing the LAr/Pb and LKr/W ECAL designs

Comparing LAr/LKr ECAL designs

- Less comprehensive analysis $\rightarrow$ goal is π^0 reconstruction results
- In order to isolate effect of smaller cells, a revised LAr/Pb design with cell size $1 \times 1 \times 4\ \mathrm{cm}^3$ is also investigated
- Clustering thresholds and reconstruction limits are kept fixed

Comparing LAr/LKr ECAL designs

- Less comprehensive analysis → goal is π^0 reconstruction results
- In order to isolate effect of smaller cells, a revised LAr/Pb design with cell size $1 \times 1 \times 4 \text{ cm}^3$ is also investigated
- Clustering thresholds and reconstruction limits are kept fixed

Challenge: Truth information of photons in SPG π^0 events is not available → some fake photons will be considered in this sub-analysis, but luckily the their influence on the results is negligible

Spatial resolution

	Initial LAr design	Revised LAr design	LKr design
$r\phi/\theta$ res.	1.28 mm	0.98 mm	0.76 mm

Table: Measured for 10 GeV photons

$\Rightarrow$ Narrower showers in LKr design improves spatial significantly

Resolved π^0 results

Initial LAr design

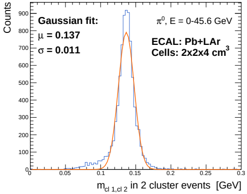

Revised LAr design

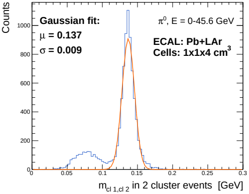

LKr design

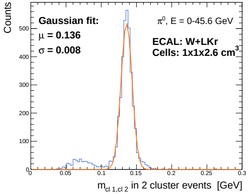

- Bumps since clustering is not optimized here. They do however not result in identification of fake π^0's
- The mass resolution is improved for both the revised LAr design and the LKr design

Unresolved π^0 results

Initial LAr design

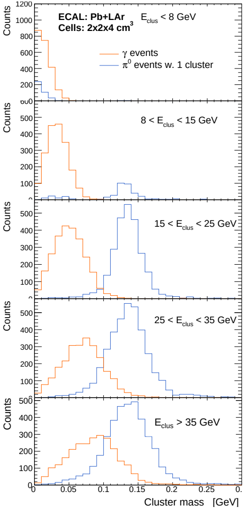

Revised LAr design

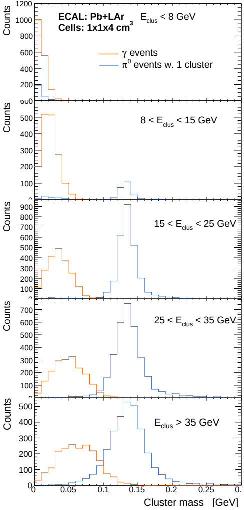

LKr design

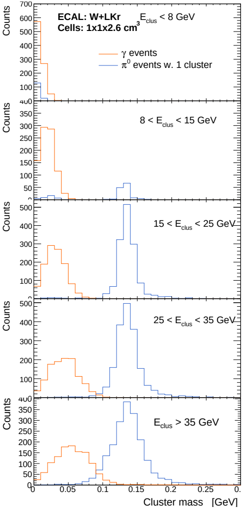

Overall π^0 reconstruction

Example: LKr design

Signal:

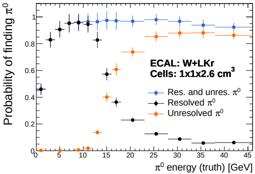

Background:

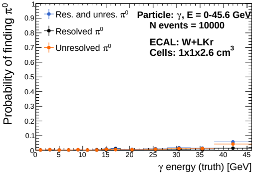

ECAL	Efficiency	
	Signal	Background
Initial LAr ECAL	89.23%	5.62%
Revised LAr ECAL	91.09%	2.48%
LKr ECAL	91.17%	1.09%

$\Rightarrow$ Reducing cell size in LAr enhances spatial resolution and improves π^0 reconstruction

$\Rightarrow$ The LKr design seems well-suited for suppressing fake π^0's

Conclusion

Conclusion

- Central detector demands for future ECAL wrt. τ polarisation measurements: fine granularity, high energy resolution and low noise levels

Conclusion

- Central detector demands for future ECAL wrt. τ polarisation measurements: fine granularity, high energy resolution and low noise levels

The LAr/Pb ECAL:

- Resolutions: $\frac{\sigma_E}{E} = \frac{8.3\%}{\sqrt{E}}$, $r\phi/\theta$: 1.28 mm

Conclusion

- Central detector demands for future ECAL wrt. τ polarisation measurements: fine granularity, high energy resolution and low noise levels

The LAr/Pb ECAL:

- Resolutions: $\frac{\sigma_E}{E} = \frac{8.3\%}{\sqrt{E}}$, $r\phi/\theta$: 1.28 mm
- Clustering: Using low (but realistic) thresholds plus reconstruction limit properly reconstructs the particles

Conclusion

- Central detector demands for future ECAL wrt. τ polarisation measurements: fine granularity, high energy resolution and low noise levels

The LAr/Pb ECAL:

- Resolutions: $\frac{\sigma_E}{E} = \frac{8.3\%}{\sqrt{E}}$, $r\phi/\theta$: 1.28 mm
- Clustering: Using low (but realistic) thresholds plus reconstruction limit properly reconstructs the particles
- The fake photon killing successfully suppresses fake photons by approximately a factor 26

Conclusion

- Central detector demands for future ECAL wrt. τ polarisation measurements: fine granularity, high energy resolution and low noise levels

The LAr/Pb ECAL:

- Resolutions: $\frac{\sigma_E}{E} = \frac{8.3\%}{\sqrt{E}}$, $r\phi/\theta$: 1.28 mm
- Clustering: Using low (but realistic) thresholds plus reconstruction limit properly reconstructs the particles
- The fake photon killing successfully suppresses fake photons by approximately a factor 26
- π^0 reconstruction eff. is $\epsilon = 84\%$ and is competitive with ALEPH results. For background: $\epsilon_{bg} = 4.5\%$

Conclusion

- Central detector demands for future ECAL wrt. τ polarisation measurements: fine granularity, high energy resolution and low noise levels

The LAr/Pb ECAL:

- Resolutions: $\frac{\sigma_E}{E} = \frac{8.3\%}{\sqrt{E}}$, $r\phi/\theta$: 1.28 mm
- Clustering: Using low (but realistic) thresholds plus reconstruction limit properly reconstructs the particles
- The fake photon killing successfully suppresses fake photons by approximately a factor 26
- π^0 reconstruction eff. is $\epsilon = 84\%$ and is competitive with ALEPH results. For background: $\epsilon_{bg} = 4.5\%$
- τ decay mode identification is generally successful with an efficiency of 96% and 90% for the $\pi^{\pm}\nu$ and $\pi^{\pm}\pi^0\nu$ channels, respectively.

Conclusion

- Central detector demands for future ECAL wrt. τ polarisation measurements: fine granularity, high energy resolution and low noise levels

The LAr/Pb ECAL:

- Resolutions: $\frac{\sigma_E}{E} = \frac{8.3\%}{\sqrt{E}}$, $r\phi/\theta$: 1.28 mm
- Clustering: Using low (but realistic) thresholds plus reconstruction limit properly reconstructs the particles
- The fake photon killing successfully suppresses fake photons by approximately a factor 26
- π^0 reconstruction eff. is $\epsilon = 84\%$ and is competitive with ALEPH results. For background: $\epsilon_{bg} = 4.5\%$
- τ decay mode identification is generally successful with an efficiency of 96% and 90% for the $\pi^{\pm}\nu$ and $\pi^{\pm}\pi^0\nu$ channels, respectively.

- The LKr/W ECAL design provides narrower showers which enhances the spatial resolution and precision in π^0 reconstruction $\Rightarrow$ future studies

Thank you for listening!

Back-up

π^0 invariant mass resolution

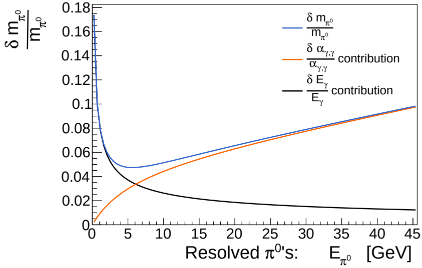

Using the assumption that $E_{\gamma,1} = E_{\gamma,2}$. Total mass resolution given by:

$$\frac{\delta m}{m} = \sqrt{\left(\frac{\delta E}{E}\right)^2 + \left(\frac{\delta \alpha_{\gamma,\gamma}}{\alpha_{\gamma,\gamma}}\right)^2} \tag{4}$$

$\Rightarrow$ Energy contribution dominant at low energies

Longitudinal profile

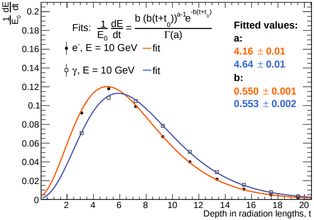

Figure: The constant $t_0 = 0.7X_0$ accounts for the depth of the cryostat and LAr pre-sampler

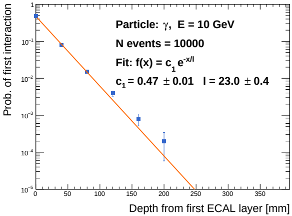

Probability of no interaction:

$$P(x) = Ce^{-x/\ell} \tag{5}$$

Expected value: $\ell = 24.99$ mm

⇒ Measured and expected profile are consistent
⇒ Electrons interact earlier (on average) than photons

⇒ Expected and calculated MFP are not consistent but close

τ polarisation measurements

The polarisation

$$P_\tau(\cos\theta) = -\frac{\mathcal{A}_\tau\left(1+\cos^2\theta\right) + 2\cos\theta\mathcal{A}_e}{\left(1+\cos^2\theta\right) + 2\mathcal{A}_\tau\mathcal{A}_e\cos\theta} \quad (6)$$

with the fermion asymmetry parameter

$$\mathcal{A}_\mathrm{f} = \frac{\left(c_L^\mathrm{f}\right)^2 - \left(c_R^\mathrm{f}\right)^2}{\left(c_L^\mathrm{f}\right)^2 + \left(c_R^\mathrm{f}\right)^2} \quad (7)$$

$$\equiv \frac{2c_V^\mathrm{f}c_A^\mathrm{f}}{\left(c_V^\mathrm{f}\right)^2 + \left(c_A^\mathrm{f}\right)^2} \quad (8)$$

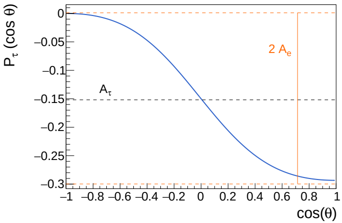

Figure: $P_\tau(\cos\theta)$ for $\mathcal{A}_\mathrm{e} = \mathcal{A}_\tau = 0.15$